

The BMP-Binding Protein Crossveinless 2 Is a Short-Range, Concentration-Dependent, Biphasic Modulator of BMP Signaling in *Drosophila*

Mihaela Serpe,^{1,2} David Umulis,^{1,3} Amy Ralston,⁴ Jun Chen,^{4,5} David J. Olson,⁴ Andrei Avanesov,^{4,5} Hans Othmer,³ Michael B. O'Connor,^{1,2,*} and Seth S. Blair^{4,*}

¹Department of Genetics, Cell Biology and Development

²The Howard Hughes Medical Institute

³School of Mathematics and Digital Technology Center
University of Minnesota, Minneapolis, MN 55455, USA

⁴Department of Zoology

⁵Genetics Training Program

University of Wisconsin, 250 North Mills Street, Madison, WI 53706, USA

*Correspondence: moconnor@umn.edu (M.B.O.), ssblair@wisc.edu (S.S.B.)

DOI 10.1016/j.devcel.2008.03.023

SUMMARY

In *Drosophila*, the secreted BMP-binding protein Short gastrulation (Sog) inhibits signaling by sequestering BMPs from receptors, but enhances signaling by transporting BMPs through tissues. We show that Crossveinless 2 (Cv-2) is also a secreted BMP-binding protein that enhances or inhibits BMP signaling. Unlike Sog, however, Cv-2 does not promote signaling by transporting BMPs. Rather, Cv-2 binds cell surfaces and heparan sulfate proteoglycans and acts over a short range. Cv-2 binds the type I BMP receptor Thickveins (Tkv), and we demonstrate how the exchange of BMPs between Cv-2 and receptor can produce the observed biphasic response to Cv-2 concentration, where low levels promote and high levels inhibit signaling. Importantly, we show also how the concentration or type of BMP present can determine whether Cv-2 promotes or inhibits signaling. We also find that Cv-2 expression is controlled by BMP signaling, and these combined properties enable Cv-2 to exquisitely tune BMP signaling.

INTRODUCTION

Extracellular ligand-binding molecules affect not only the range and stability of signals in the extracellular space, but often supply spatial or timing information critical for patterning developmental events (Lander, 2007). The secreted Crossveinless 2 (Cv-2) protein, first discovered in *Drosophila*, is required for signaling by the bone morphogenetic protein (BMP) homologs Dpp and Gbb during formation of *Drosophila* wing crossveins (Conley et al., 2000). Vertebrates have Cv-2 homologs (also called BMPER) and related proteins (Kielin) that also modulate BMP signaling (reviewed in O'Connor et al., 2006). All contain N-terminal cysteine-rich (CR) domains that are strongly similar to the BMP-binding regions of vertebrate Chordin and its *Drosophila* homolog Sog, and

a C-terminal von Willebrand Factor D (vWFD) domain. However, the mechanism by which Cv-2 and its relatives modulates BMP signaling is not clear.

As in the *Drosophila* wing, loss-of-function studies in zebrafish and mice indicate that Cv-2 and Kielin-like proteins promote BMP signaling in certain contexts (Ikeya et al., 2006; Moser et al., 2007; Rentzsch et al., 2006). But while increasing the levels of Cv-2 or Kielin-like proteins can promote BMP signaling in some assays, in others increasing Cv-2 inhibits signaling (Binnerts et al., 2004; Coles et al., 2004; Kamimura et al., 2004; Lin et al., 2005, 2006; Matsui et al., 2000; Moser et al., 2003; Ralston and Blair, 2005; Rentzsch et al., 2006). Any proposed mechanism of action must therefore explain these contradictory effects.

The ability of Cv-2 either to promote or inhibit signaling is reminiscent of the dual activities of Sog and Twisted gastrulation (Tsg) (reviewed in O'Connor et al., 2006). Sog and Tsg form a complex that binds and sequesters BMPs to inhibit signaling in the ventrolateral regions of the early *Drosophila* embryo. However, Sog and Tsg also promote accumulation of BMPs and heighten BMP signaling in the dorsal-most cells of the embryo, distant from the site of Sog expression (Shimmi et al., 2005b; Wang and Ferguson, 2005). Evidence suggests that Sog and Tsg promote signaling via a transport mechanism; BMPs bound to the Sog-Tsg complex move over a longer range, likely because they are protected from binding to receptors and other cell surface proteins. In dorsal cells, the Tolloid metalloprotease cleaves Sog, enabling BMPs to bind receptors and signal.

Intriguingly, Sog-mediated BMP transport is also likely required for BMP signaling during formation of the crossveins in the *Drosophila* wing, the process affected by Cv-2. Specification of the posterior crossvein (PCV) from the ectodermal epithelium of the pupal wing is presaged by localized activation of BMP signaling, and loss of BMP signaling causes a crossveinless phenotype (Conley et al., 2000). Several studies have suggested that Dpp and Gbb ligands move from the longitudinal veins into the PCV region (Ralston and Blair, 2005; Ray and Wharton, 2001), and that Sog, a second member of the Tsg family named Crossveinless (Cv), and the Tolloid-related (Tlr) protease are required

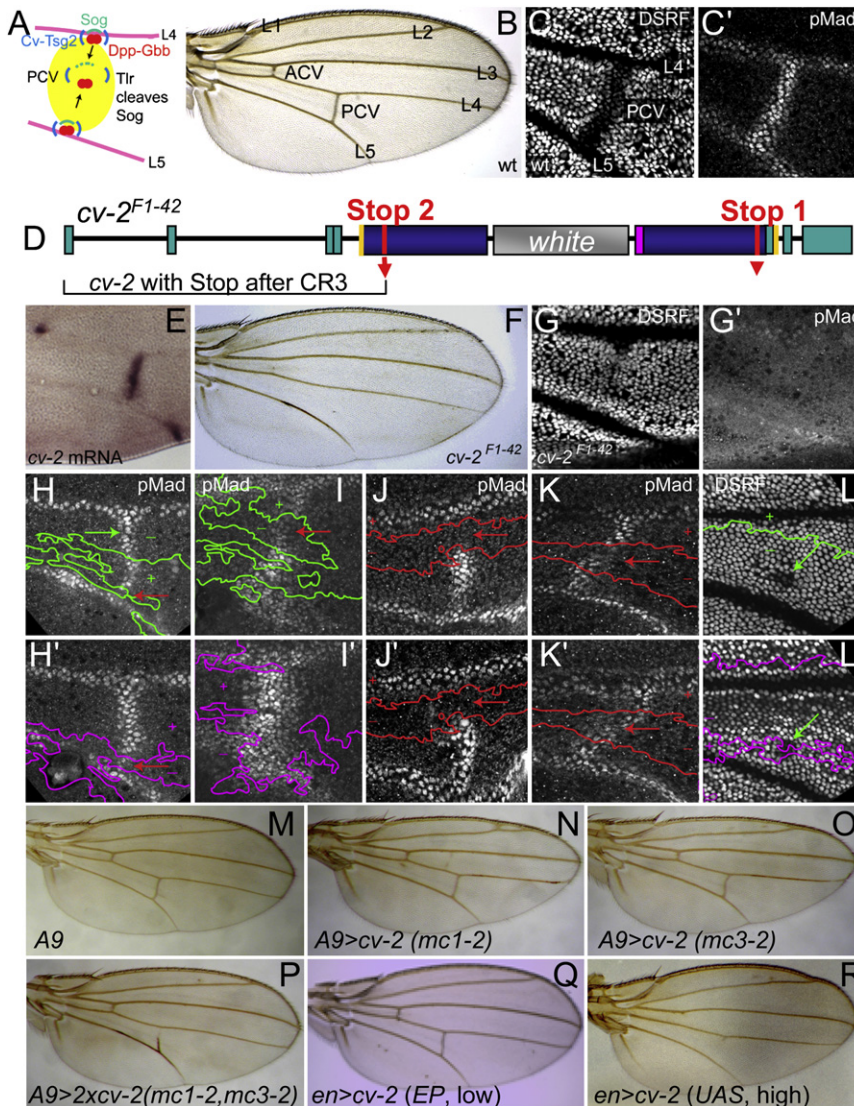


Figure 1. The Nature and Range of Cv-2 Function

(A) Model of BMP signaling in the developing PCV. (B) Wild-type adult wing. (C and C') DSRF and pMad levels in the wild-type pupal PCV. (D) Diagram of the *cv-2^{F1-42}* allele created by targeted mutagenesis. (E) *cv-2* mRNA in the pupal crossvein region. (F) *cv-2^{F1-42}* adult wing. (G and G') DSRF and pMad in pupal *cv-2^{F1-42}* PCV. (H-L) Effect of homozygous *cv-2^{F1-42}* clones on pMad (H-K') or DSRF (L and L') in pupal wings. Panels show both surfaces of the PCV region with corresponding clones (green or magenta outlines) or, in (J)-(K'), the region of clone overlap (red outlines). Wild-type sides of the boundaries are marked + and mutant -. Arrows mark regions of clones with normal (green) or disrupted (red) development of the PCV. (M) Adult *A9-gal4* wings. *A9-gal4* is expressed throughout the pupal wing, at levels lower than that of *en-gal4* (data not shown). (N-P) Overexpression of a single copy (N and O) or two copies (P) of *UAS-cv-2* with *A9-gal4* (N and O). (Q) Overexpression of low levels of *cv-2* with *en-gal4* and *EP-driven cv-2* (*EP(2)1103*). (R) Overexpression of high levels of *cv-2* with *en-gal4* and *UAS-cv-2*. The posterior-specific *en-gal4* driver is expressed throughout most of the ACV region, ending just posterior to L3 (Ralston and Blair, 2005).

RESULTS

Endogenous Cv-2 Acts over a Short Range to Augment BMP Signaling in the PCV

To more completely investigate *cv-2* function, we generated new *cv-2* alleles by targeted recombination, with predicted truncations after the second (*cv-2^{KO2}*) or third (*cv-2^{F1-42}*, *cv-2^{KO1}*) CR domains (Figure 1D; Figure S1, see the Supplemental Data available with this article online). These alleles produced identical phenotypes and are likely functional nulls. All could be maintained as homozygotes, and thus neither maternal nor zygotic *cv-2* is essential for embryogenesis, although significant parate lethality is observed at 18°C. Wing phenotypes were identical to those of hypomorphs (Conley et al., 2000): adult wings lacked the PCV and sometimes the anterior crossvein (ACV) and the tips of some longitudinal veins (compare Figures 1B and 1F). BMP signaling, marked by phosphorylation of the receptor-activated Smad Mad (pMad), was lost or reduced in the developing crossveins, while expression of the intervein marker DSRF was heightened (compare Figures 1C and 1C' to 1G and 1G'). BMP signaling in the longitudinal veins was also slightly reduced or delayed.

To examine the range over which Cv-2 acts, we examined the effects of homozygous *cv-2^{F1-42}* clones on pMad and DSRF. The pupal wing has closely apposed dorsal and ventral epithelia,

for this movement and subsequent signaling (Serpe et al., 2005; Shimmi et al., 2005a; Vilmos et al., 2005; Figure 1A).

In this report we show that Cv-2 acts via a very different mechanism. While Cv-2 binds Dpp and Gbb, it does not help transport them from the longitudinal veins. Rather, it acts over a very short range within the PCV, likely because it binds to cell surface heparan sulfate proteoglycans (HSPGs). Moreover, we show that Cv-2 binds to the BMP type I receptor Tkv. We combine computational and experimental strategies to show that the exchange of BMPs between Cv-2 and Tkv can either stimulate or inhibit signaling. Raising Cv-2 levels can convert Cv-2 from an agonist to an antagonist of signaling, and this "biphasic" activity is influenced by the concentration and even the types of BMPs present. We also show that the ability of *Drosophila* Cv-2 to promote BMP signaling does not require the cleavage of Cv-2, in contrast to a model recently proposed for zebrafish Cv-2 (Rentzsch et al., 2006). Finally, we show how positive regulation of *cv-2* expression by BMP signaling can sharpen the boundary between regions of high and low BMP signaling.

and most clones that are restricted to one surface do not block PCV formation on either surface of the wing, suggesting that Cv-2 can diffuse from the normal to the mutant wing surface to rescue crossvein formation (Figures 1H–1L'). However, a minority of single-sided clones showed reduced anti-pMad staining (Figures 1I and 1I') or heightened anti-DSRF staining (data not shown). When clones on opposite surfaces of the wing overlapped more than two to three cell diameters, BMP signaling and DSRF expression were always disrupted (overlapping regions in red in Figures 1J–1K'; see Figures S2A–S2E). Adjacent wild-type cells rescued signaling and PCV formation over at most two to three cell diameters. Importantly, Cv-2 activity was only required within the PCV; mutant clones that overlapped the PCV but did not overlap the longitudinal veins still blocked signaling in the PCV (Figures 1J–1K'), and wild-type cells wholly within the PCV could rescue PCV formation in immediately adjacent cells on both surfaces (Figure 1L and Figure S2E). In contrast, Sog or Cv must be removed from large portions of the wing to block PCV formation (Shimmi et al., 2005a; Figure S2F). We conclude that Cv-2 does not transport Dpp from the longitudinal veins into the crossvein region. Rather, Cv-2 is required around or in the PCV cells receiving the BMP signal. This conclusion is consistent with the heightened expression of *cv-2* within the forming PCV (Conley et al., 2000; Figure 1E).

Overexpression of Cv-2 Can Inhibit BMP Signaling

Intriguingly, we found that overexpression of Cv-2 could either augment or antagonize BMP signaling during wing development, depending on the levels being expressed. When we overexpressed moderate levels of Cv-2 in the developing wing with *A9-gal4* and a single copy of *UAS-cv-2*, the PCV formed normally with occasional formation of additional veins indicative of a slight gain in signaling (Figures 1M–1O). These levels of expression also rescued PCV formation in homozygotes of the hypomorph *cv-2¹* or the null *cv-2^{KO1}* (see below). However, driving higher levels of expression using two copies of *UAS-cv-2* with *A9-gal4* partially blocked PCV formation (Figure 1P). Similarly, *en-gal4* drives moderate expression of *cv-2* from the *EP(2)1103* *UAS* insertion located upstream of *cv-2*, causing only slight expansion of anti-pMad staining in the PCV and the formation of normal adult PCV (Conley et al., 2000; Ralston and Blair, 2005), but driving higher levels using *en-gal4* and *UAS-cv-2* blocked PCV formation in pupal (data not shown) and adult wings (Figures 1Q and 1R; expression levels are compared in Figure S3). Thus, BMP signaling shows a biphasic response to changes in Cv-2 levels: low signaling without Cv-2, maximum signaling with wild-type or moderate misexpression of Cv-2, and then decreased signaling with strong misexpression of Cv-2.

Cv-2 Is Cleaved into CR and vWFD Domains that Remain Associated via Disulfide Bonds

We next explored some of Cv-2's biochemical features by examining Cv-2 variants with N-terminal 6×Myc and/or C-terminal V5/6His tags (Figure 2A). Supernatant from cells overexpressing dual-tagged Cv-2 contained full-length protein (120 kDa) as well as 65 kDa N-terminal and 55 kDa C-terminal fragments (Figure 2B), indicating that Cv-2 is secreted from S2 cells as a mixture of full-length and cleaved products. A comparable mixture of cleaved and uncleaved forms was found after expression of tagged constructs in embryos using *da-gal4* (Figure 2C). Similar

processing has been reported for vertebrate Cv-2 homologs (Binnerts et al., 2004; Kamimura et al., 2004; Moser et al., 2003; Rentzsch et al., 2006).

The N-terminal sequence of the 55 kDa C-terminal fragment purified from S2 cell supernatant was PHFRTFDGKGF. Thus, the main cleavage site lies between GD³⁸⁸ and P³⁸⁹H at the beginning of the vWFD domain. This is identical to the cleavage site utilized in zebrafish Cv-2 (Rentzsch et al., 2006) and is conserved, along with the surrounding amino acids, in all Cv-2-like proteins (Figure 2D). Mutating G³⁸⁷DP to AAA (Cv-2^{Un}) blocked cleavage in vitro (Figure 2E) and in embryos (Figure 2F). Removing the GD-PH site along with the rest of the vWFD domain also blocked cleavage in vitro (Cv-2-N; Figure 2E).

N-terminal and C-terminal cleavage fragments of Cv-2 are linked by a disulfide bond, because the mobility of both fragments shifted to that of the full-length protein under nonreducing electrophoretic conditions (compare reducing [R] and nonreducing [N] lanes in Figure 2E). Similar results have been observed for vertebrate Cv-2 homologs (Binnerts et al., 2004; Rentzsch et al., 2006). We confirmed association between these fragments by coimmunoprecipitation (IP) using dual-tagged Cv-2 (Figure 2G).

The only cysteine remaining in the N-terminal fragment of Cv-2 (C³⁸³) still binds the C-terminal fragment (Figure 2E). Work on human vWFD (Marti et al., 1987) suggests C³⁸³ should cross-link with C⁵²⁰. Interestingly, mutating C³⁸³ or C⁵²⁰ to A blocked Cv-2 cleavage, while cleavage still occurred after mutating the other cysteines in the first half of the vWFD domain (Figure 2H) or removing the second half of the vWFD domain (data not shown). Thus, the disulfide link between the two halves of Cv-2 likely imposes a conformational change that is required for cleavage, and therefore precedes it.

Cv-2 Binds Dpp and Gbb

Flag-tagged Dpp and Gbb both IP Cv-2 in vitro (Figure 2I). Comparison of Cv-2 levels in the input and output revealed that full-length Cv-2 was more highly concentrated than the processed form. While the input contained higher levels of cleaved Cv-2, higher levels of uncleaved Cv-2 precipitated with Dpp (highest levels shown by blue in Figure 2J; levels quantified in Figure 2K). Thus, processing appears to reduce the affinity of Cv-2 for ligand in this assay.

The CR domains of zebrafish Cv-2 can bind BMPs (Rentzsch et al., 2006; Zhang et al., 2007), and, as expected, a form of *Drosophila* Cv-2 lacking the CR domains (Cv-2-C) did not co-IP with tagged BMPs in vitro (Figure 2L). However, a form of Cv-2 lacking the vWFD domain (Cv-2-N) also did not co-IP with BMPs (Figure 2L). Thus the vWFD domain enhances BMP binding to the CR domains, possibly by regulation of protein conformation or through other proteins.

Cv-2 Binds to *Drosophila* HSPGs through GAG Chains

The short-range action of endogenous Cv-2 suggested that Cv-2 interacts with the cell surface or extracellular matrix. Indeed, naive S2 cells bound a fraction of both full-length and cleaved Cv-2, even if incubated at 4°C to inhibit endocytosis (Figures 3A and 3B). This binding is likely mediated by the vWFD domain, as S2 cells bound Cv-2-C, which contains only the vWFD domain, but failed to bind Cv-2-N, which contains only the CR domains (Figures 3A and 3B).

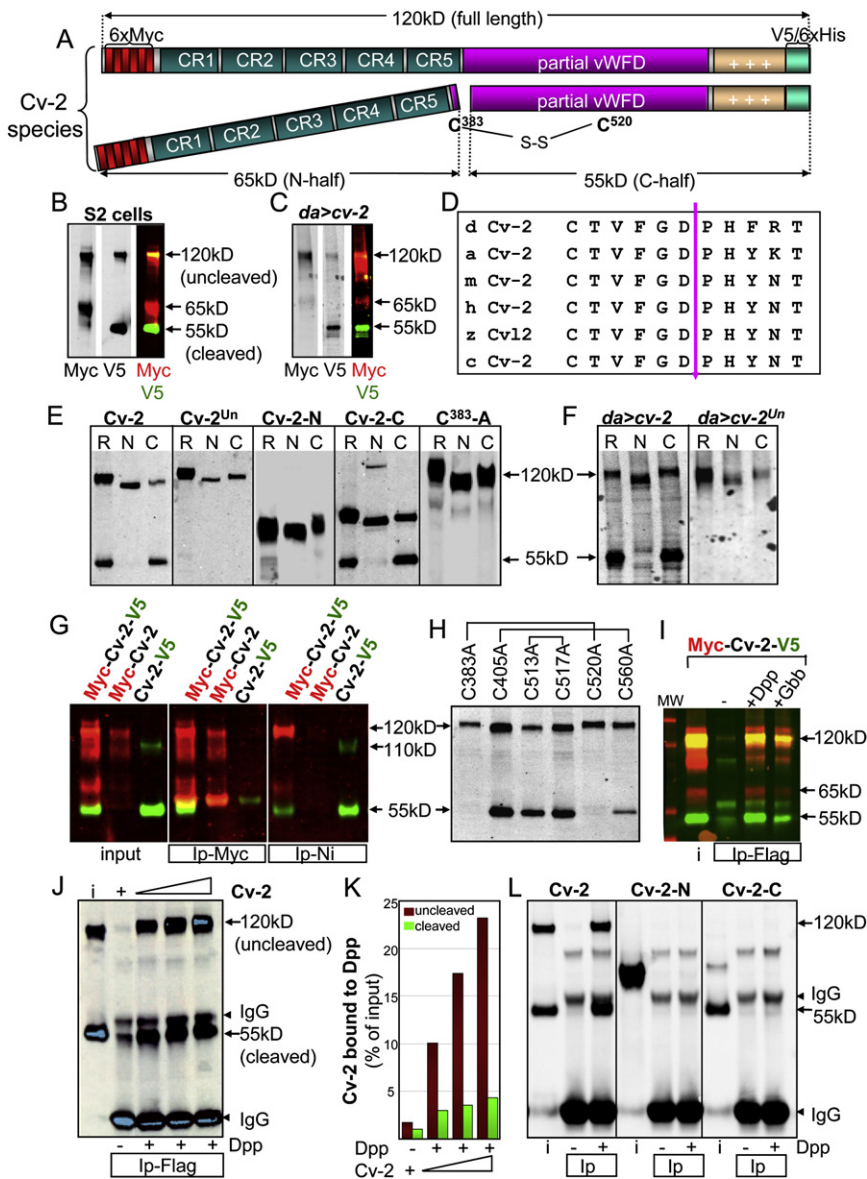


Figure 2. Biochemical Characterization of *Drosophila* Cv-2

(A) Diagram of dual-tagged Cv-2 proteins (6×Myc N-terminal and V5-6×His C-terminal) showing CR and vWFD domains, and cleavage and disulfide bonding between N-terminal and C-terminal fragments. All the Cv-2 variants used below were similarly tagged with C-terminal V5-6×His and, in some cases, N-terminal 6×Myc.

(B, C, E–J, and L) Western analyses of tagged Cv-2. The immunoblots in (B), (C), (G), and (I) show simultaneous anti-Myc (red) and anti-V5 (green) staining; in the rest of the panels only anti-V5 staining is shown.

(B and C) Dual-tagged Cv-2 produced in S2 cells (B) or in embryos after overexpression of *UAS-cv-2* with *da-gal4* (C).

(D) Conservation of the cleavage site in Cv-2 proteins (d, *Drosophila*; a, *Anopheles*; m, mouse; h, human; z, zebrafish; c, chicken).

(E) Cleavage and mobility shifts for Cv-2 variants from S2 cell supernatant under reducing (R) and nonreducing (N) conditions, or from S2 cell pellets (C) run under reducing conditions. The slightly faster migration of full-length Cv-2 under nonreducing conditions is likely due to conformational changes.

(F) Cleavage and mobility shifts for dual-tagged wild-type and uncleavable ($G^{387}DP-AAA$) *cv-2* variants overexpressed in embryos with *da-gal4*, run under reducing (R) and nonreducing (N) conditions.

(G) IP of dual-tagged Myc-Cv-2-V5/6His with either anti-Myc (center western) or Ni (right western) co-IPs the N-terminal or C-terminal fragment of Cv-2, respectively. Control lanes show the absence of precipitation of single-tagged Cv-2-V5/6His by anti-Myc or of Myc-Cv-2 by Ni beads. Full-length Myc-tagged Cv-2 runs at 120 kDa, Cv-2-V5/6His at 110 kDa.

(H) Cv-2 cleavage requires C^{383} and C^{520} , but not C^{405} , C^{513} , C^{517} or C^{560} . Predicted Cys pairings in the first half of the vWFD domain are indicated.

(I) Cleaved and uncleaved forms of the dual-tagged Myc-Cv-2-V5 coprecipitate with Dpp-Flag or Gbb-Flag, but not with the anti-Flag-beads alone (–). i, input Cv-2.

(J) Levels of cleaved and uncleaved Cv-2 that co-IP with Dpp-Flag, compared with input levels (highest levels shown in blue).

(K) Relative amounts of cleaved and uncleaved Cv-2 that co-IP with Dpp-Flag, expressed as the percentage of the input levels.

(L) Full-length Cv-2, but not Cv-2-N or Cv-2-C, co-IPs with Flag-tagged Dpp.

Many extracellular molecules bind to cell surface HSPGs, such as the *Drosophila* Glypican Dally (reviewed in Lin, 2004). We found that S2 cells overexpressing Dally accumulated much higher levels of Cv-2 on their surface than did untransfected cells (Figure 3C). This binding appears to be mediated by the vWFD domain, since Cv-2-C, but not Cv-2-N, bound Dally-expressing cells (Figures 3D and 3E). Moreover, Myc-tagged Dally co-IPs both full-length and cleaved Cv-2 (Figure 3F). This Dally-Cv-2 interaction was unaffected by the presence of Dpp or by blocking endocytosis at 4°C.

The binding of many proteins to HSPGs is mediated by Glycosamino Glycan (GAG) side chains, and we found that removing GAGs reduced accumulation of Cv-2 on cell surfaces in vivo. We expressed Myc-tagged Cv-2 with the *A9-gal4* driver in wing discs containing clones lacking Brother of tout-velu (*Botv*), an EXT polymerase required for GAG formation (Han et al., 2004; Takei et al., 2004). The levels of extracellular Cv-2, visualized by applying anti-Myc prior to fixation (Strigini and Cohen, 2000), were substantially lower in *botv* mutant clones (Figure 3G). Clones lacking Dally and the Dlp Glypican also block signaling in the PCV (data not shown),

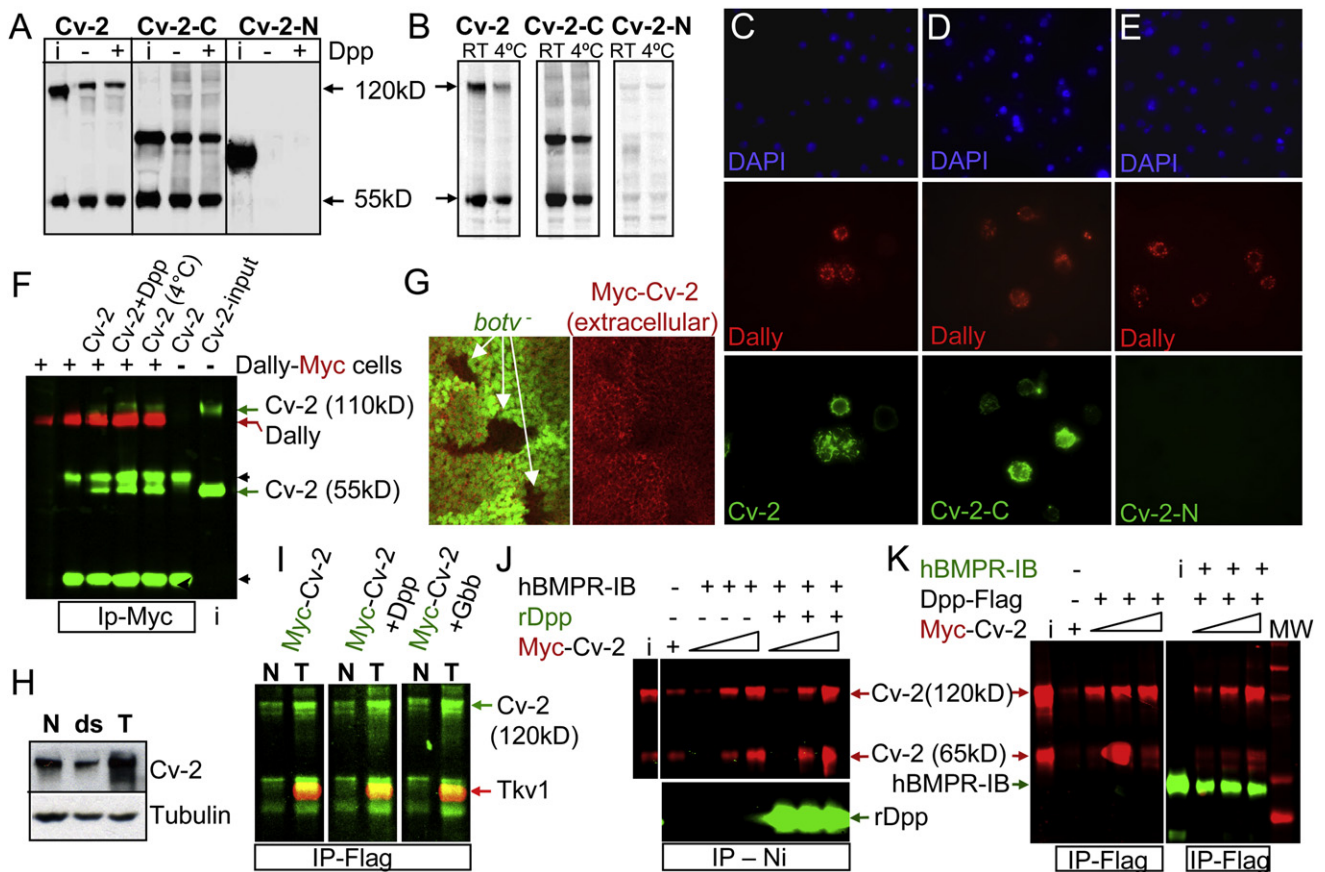


Figure 3. Cv-2 Interacts with the Cell Surface, Dally, and the BMP Type I Receptor Tkv

(A and B) Binding of Cv-2 and Cv-2-C, but not Cv-2-N, to naive S2 cells. i, input lanes. Binding is not influenced by the addition of Dpp (+ versus –) (A), and occurs at both room temperature (RT) and 4°C (B).

(C–E) Increased binding of V5-tagged Cv-2 and Cv-2-C, but not Cv-2-N (anti-V5 in green), from S2 cell supernatant to S2 cells overexpressing Myc-tagged Dally (anti-Myc in red). DAPI (blue) stains the nuclei of transfected and untransfected cells.

(F) Cv-2 (green) co-IPs with Myc-tagged Dally (red). Black arrowheads, IgG bands.

(G) Reduced extracellular accumulation of *A9-gal4*-driven Myc-Cv-2 (anti-Myc, red) in *botv* clones, marked by the absence of a GFP (green) marker, in wing imaginal discs.

(H) Comparison of Cv-2 binding to identical numbers of naive (N), *tkv* dsRNA (ds), and *tkv*-transfected (T) S2 cells. Anti-tubulin is shown as a loading control. On average a 50% decrease was seen in five dsRNA repetitions.

(I) Cv-2 co-IPs with Flag-tagged Tkv. While there is some background IP of Myc-Cv-2 (green) in naive cells (N), the level of IP is increased 4- to 7-fold in cells (five repetitions) expressing Tkv1 (T) and is not affected by the addition of Dpp or Gbb.

(J) *Drosophila* Cv-2 co-IPs with a His-tagged chimera containing the extracellular domain of human BMPR-IB, with or without recombinant Dpp (green).

(K) Dpp-Flag simultaneously IPs Myc-Cv-2 (red) and a His-tagged Fc-chimera containing the extracellular portion of BMPR-IB (green). In (J) and (K): i, input proteins; + in Myc-Cv-2 lanes indicates maximal levels; MW, molecular weight marker.

although this may be due as much to the loss of extracellular Dpp (Belenkaya et al., 2004) as to the loss of Cv-2 surface binding.

Cv-2 Associates with the BMP Receptor Tkv

One way that Cv-2 might augment signaling is by promoting cleavage of Sog by Tolloid-like proteases, releasing BMPs for signaling. However, we could not detect any increase in the cleavage of BMP-bound Sog by Tld or Tlr after the addition of Cv-2 (data not shown). Alternatively, Cv-2 might act at the level of the BMP receptors, and we found that Cv-2 could associate with the BMP type I receptor Tkv. S2 cells express endogenous Tkv, and lowering *tkv* levels by RNAi diminished the amount of Cv-2 bound to cells, while overexpression of *tkv* led to an

increase in bound Cv-2 (Figure 3H). Binding of uncleavable Cv-2 was also sensitive to Tkv levels, but binding of Cv-2-C was not (Figure S4). The Cv-2/Tkv interaction thus differs from the Cv-2/HSPG interaction, which does not require the CR domains (Figures 3A–3E). Accumulation of extracellular Cv-2 in wing imaginal discs was similarly sensitive to alterations in Tkv levels (Figure S5). We also found that tagged Tkv expressed in S2 cells could co-IP Cv-2 (Figure 3I). This binding was not obviously altered by the addition of Dpp or Gbb.

Since *Drosophila* Cv-2 can substitute for vertebrate Cv-2 in zebrafish (Rentzsch et al., 2006), we also examined interactions with a vertebrate type I BMP receptor. Cv-2 bound constructs containing the extracellular portion of vertebrate BMPR-IA or -IB, and this binding was not inhibited or enhanced by the

addition of Dpp (BMPP-IB in Figure 3J; BMPP-IA is not shown). Cv-2 did not bind the extracellular domains of either vertebrate BMPP-II or the non-TGF- β Erb-B2, indicating that the interaction with the type I receptor is specific (Figure S4B). We also found that Dpp could simultaneously co-IP both Cv-2 and Fc-BMPP-IB (Figure 3K), suggesting that Dpp, Cv-2, and the type I receptor can form a tripartite complex.

A Kinetic Model for Biphasic Modulation of BMP Signaling by Cv-2

To understand how interactions between Cv-2, BMPs, and BMP receptors could generate a biphasic Cv-2 dose-response curve, we constructed a model that incorporates binding among Cv-2, BMP ligands, and receptors (Figure 4A). Because of the short-range action and HSPG binding of Cv-2, we assume that Cv-2 acts locally and regulates BMP signaling autonomously. The local dynamics for the model incorporates BMP (*B*) binding to Cv-2 (*C*), BMP binding to receptor (*R*), and the transfer of bound BMP between the Cv-2 complex (*BC*) and the BMP-receptor complex (*BR*) through a transient BMP/Cv-2/receptor complex (*BCR*). For simplicity, we assume that all surface-localized factors are internalized at the same rate and that the higher order signaling complex with type II receptors equilibrates rapidly, making signaling directly proportional to the level of occupied type I receptors (Umulis et al., 2006).

$$\text{BMP/Cv-2: } \frac{d[BC]}{dt} = k_1[B][C] - k_{-1}[BC] - k_3[BC][R] + k_{-3}[BCR] - \delta_E[BC] \quad (1)$$

$$\text{BMP/Cv-2/Receptor: } \frac{d[BCR]}{dt} = k_3[BC][R] + k_4[BR][C] - k_{-3}[BCR] - k_{-4}[BCR] - \delta_E[BCR] \quad (2)$$

$$\text{BMP/Receptor: } \frac{d[BR]}{dt} = k_2[B][R] - k_{-2}[BR] + k_{-4}[BCR] - k_4[BR][C] - \delta_E[BR] \quad (3)$$

$$\text{Conservation conditions: } [C_T] = [C] + [BC] + [BCR]; \\ [R_T] = [R] + [BR] + [BCR]$$

To delineate between plausible mechanisms for Cv-2 regulation of BMP signaling, three “extreme” submodels were examined (Figure 4B): (i) only *BCR* can signal (coreceptor model), (ii) *BCR* and *BR* can signal with equal strength (stabilizing factor model), and (iii) only *BR* can signal (transfer factor model). While kinetic data is available for the binding of BMPs to vertebrate type I receptors (Hatta et al., 2000; Sebald et al., 2004) and zebrafish Cv-2 (Rentzsch et al., 2006), we did not assume these values a priori. Rather, we used a large-scale parameter screen and sorted solutions based on their ability to recapitulate the biphasic response of signaling to changes in Cv-2 levels. Submodels (i) and (ii) exhibited purely agonistic responses to Cv-2 over the range of parameter sets used (example curves shown in Figure 4B). Only model (iii) was capable of generating a biphasic response: 78% of parameter sets gave rise to a purely antagonistic response (Figure 4Biii a), while 22% gave rise to a biphasic response (Figures 4Biii b and 4C). The biphasic response to

changes in the concentration of Cv-2 qualitatively recapitulates our experimental observations: loss of BMP signaling after loss of Cv-2, normal signaling after moderate increases in Cv-2, and loss of signaling after extreme increases in Cv-2 (Figure 4C).

This model makes two important points. First, the ability of high levels of Cv-2 to antagonize signaling requires that signaling mediated by a tripartite complex is compromised in comparison to the BMP-receptor complex. Second, low levels of Cv-2 should stimulate signaling without increasing the receptor’s affinity for BMPs and without forming a *BCR* complex with intrinsically higher activity. Rather, gains in signaling would result simply from the transfer of BMP from Cv-2 to the receptor via the Cv-2-receptor intermediate (*BC* to *BR* via *BCR*). This could be a very transient interaction, not requiring the formation of a high-affinity complex, and this is consistent with our observation that addition of BMPs did not enhance binding between Tkv and Cv-2.

The Response to Cv-2 Depends on BMP Levels

Computational analysis suggested that Cv-2 levels that do not inhibit the signaling induced by low, endogenous levels of BMPs could nonetheless inhibit the heightened signaling caused by overexpression of BMPs. The model predicts that BMP overexpression increases the level of signaling (*BR*) for each level of Cv-2 (compare dashed and solid lines in Figure 4D). At endogenous levels of Cv-2, this increases signaling (*a* \rightarrow *b* in Figure 4D), but coexpression of Cv-2 reduces signaling back to wild-type levels (*b* \rightarrow *c* in Figure 4D). This matches our *in vivo* results. Moderate levels of Cv-2 expression driven with *A9-gal4* and a single copy of *UAS-cv-2*, caused slight gains in venation and therefore signaling (Figures 1N and 1O), but rescued the phenotypes caused by Dpp or Gbb overexpression (Figure 4E).

Cv-2 Activity Can Depend on Specific BMPs

We next cataloged the model parameters into groups based upon their ability to lead to a biphasic response to Cv-2. The equations were nondimensionalized by the total amount of receptor (R_T) for concentration and (δ_E) for time. Typically, dissociation constants (K_D) are reported with units of concentration; however, we found that parameter segregation into classes was better captured by the dimensionless dissociation constants. Solutions were sorted according to four dimensionless forms of the K_D constants: (1) binding of BMP to Cv-2 (k_{-1}/k_1B or K_C), (2) binding of BMP to receptor (k_{-2}/k_2B or K_R), (3) binding of *BC* to *R* to yield *BCR* (k_{-3}/k_3R_T), and (4) binding of *BR* to *C* to yield *BCR* (k_{-4}/k_4R_T or K_{BCR}). Biphasic solutions favored certain regions for all K_D values except for k_{-3}/k_3R_T (Figure S6). Affinities were plotted in 3D coordinate space where the x axis corresponds to $1/K_C$, the y axis to $1/K_R$, and the z axis to $1/K_{BCR}$. The solution space was divided up into eight regions that correspond to parameters with similar biological activity based on their dimensionless K_D constants. A threshold value of 10 nM was used for sorting, such that K_D values less than 10 nM were considered high affinity (H), whereas K_D values greater than 10 nM were considered low affinity (L). The K_D threshold constants were nondimensionalized by the means of the *B* and R_T distributions accordingly (1 and 316 nM, respectively), and solutions for 10,000 sets of randomly chosen parameters for submodel (iii) along with thresholds planes are shown in

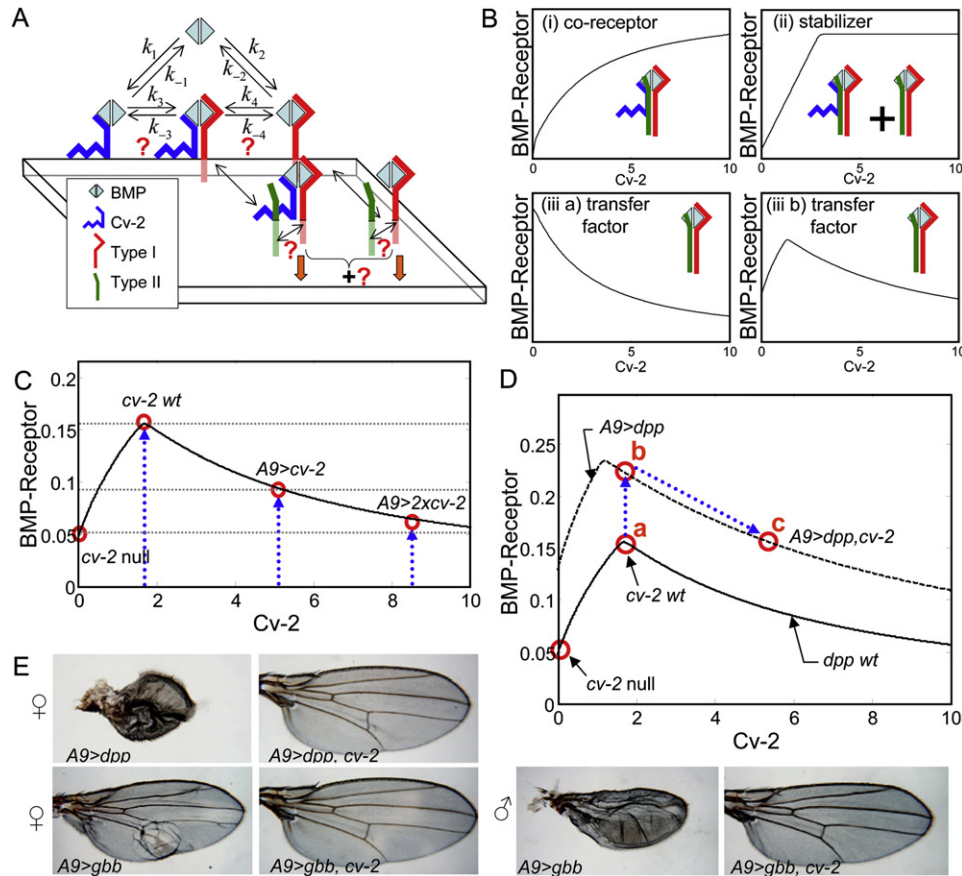


Figure 4. Modeling the Biphasic Activity of Cv-2

(A) Model for cell autonomous action of Cv-2.

(B) Typical results for three versions of the model shown in (A), with signaling possible via *BCR* only (Bi), equal signaling via *BCR* and *BR* (Bii), or signaling via *BR* only (Biii).

(C) Model results showing a biphasic response to Cv-2 levels. See Table S1 for parameter values.

(D) Model results showing how similar levels of Cv-2 overexpression can still promote signaling but suppress the effects of 3-fold increases in BMP. See Table S1 for parameter values.

(E) Overexpression of Cv-2 suppresses the effects of Dpp and Gbb overexpression on adult wings.

Figures 5A and 5B (biphasic = red; antagonistic = green). Twenty-eight percent of LLL (BMPs having low affinity [high K_D] for Cv-2, low affinity for receptor, and low affinity for the intermediate state), 66% of HLL, and 46% of HLH solutions exhibited a biphasic activity (Figure 5C). The highest percentage of biphasic solutions thus occurs when a BMP molecule has a high affinity for Cv-2, a low affinity for receptor, and a relatively low affinity for the intermediate state. Since the intermediate kinetic rates are unknown, solutions can also be sorted by Cv-2/BMP affinity and receptor/BMP affinity. Here, 56% of all solutions that have a high Cv-2 and low receptor affinity are biphasic, whereas only 16% of the solutions with high Cv-2 and high receptor affinity are biphasic (Figure 5C inset). Biphasic solutions were rare when a BMP molecule had a higher affinity for the receptor than for Cv-2.

One interesting implication of our model is that ligands that have different affinities for the receptor or Cv-2 might differ in their response to Cv-2. That is, Cv-2 might act in a biphasic manner with one ligand, but in an antagonistic manner with another.

This can occur even if the BMPs have the same affinity for Cv-2 but have different affinities for their receptors. Binding parameters between purified vertebrate homologs of *Drosophila* Dpp (BMP-2/4), Gbb (BMP-7), Tkv (BMP-1A), and zebrafish Cv-2 have been published (Hatta et al., 2000; Rentzsch et al., 2006; Sebald et al., 2004; Figure 5D). Using binding parameters for BMP-2 to the BMP-1A receptors and zebrafish Cv-2, and varying unknown parameters for K_{BCR} , yielded a biphasic response only 24.5% of the time, with the majority of the solutions exhibiting a purely antagonistic response. Furthermore, rare biphasic solutions conferred only very weak agonist activity; a typical result is shown in Figure 5E. In contrast, BMP-7 has a lower affinity for the type 1 receptor (Sebald et al., 2004) but an affinity for Cv-2 nearly as high ($K_D = 3.5$ nM) as that of BMP-2 ($K_D = 1.4$ nM) (Rentzsch et al., 2006). Choosing a K_D value for BMP-7-receptor binding from the upper end of the measured 10–100 nM range ($K_D = 100$ nM used) yielded a biphasic response to Cv-2 40% of the time, and the predicted dose-response curve was strongly biphasic over a wide range of Gbb concentrations (Figure 5F).

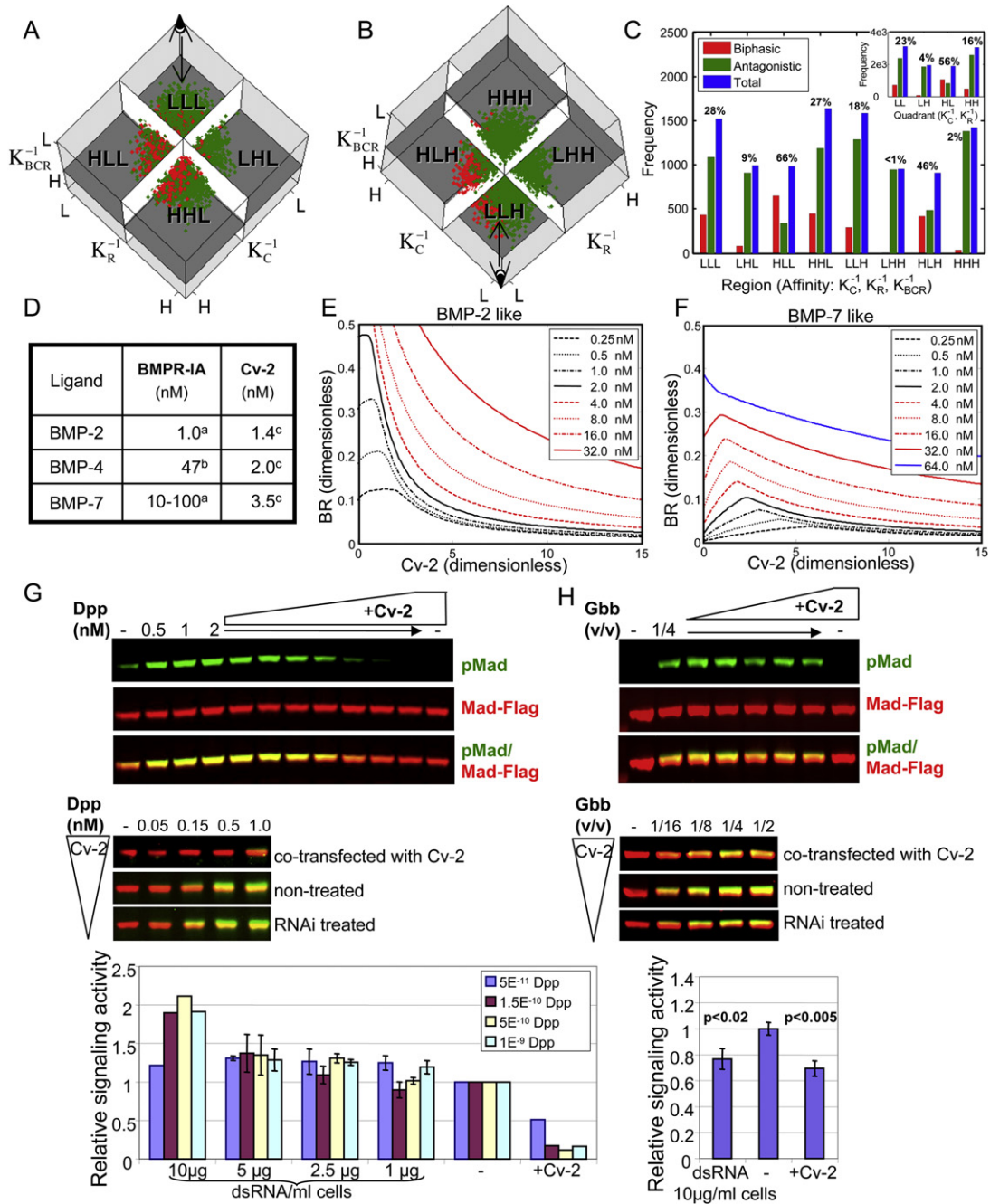


Figure 5. Biphasic Activity of Cv-2 Is Ligand Dependent

(A and B) Conditions that lead to biphasic activity of Cv-2. 10,000 results for model (iii) with randomly varying parameters are shown. The x, y, and z axes correspond to the dimensionless affinity constants for C, R, and BCR. Red dots represent biphasic solutions; green dots represent antagonistic solutions. The nondimensional thresholds were computed by adjusting by the mean R_{tot} or B used in the numerical screen, which gave values of 10, 10, and 0.0316 for K_C^{-1} , K_R^{-1} , and K_{BCR}^{-1} , respectively. Thresholds are shown by planes that dissect the data for K_C , K_R , and K_{BCR}^{-1} . Regions are denoted by three letters that correspond to (H)igh or (L)ow Cv-2 affinity, receptor affinity, and BCR affinity. (A) Top view shows solutions for $K_{BCR} > 0.0316$ (dimensionless) and four regions HHL, HLL, LLL, and HLL. (B) Bottom view with four regions: HHH, HLH, LLH, and HLH.

(C) Histogram shows number of biphasic, antagonistic, and total solutions and the percent of biphasic solutions in each region.

(D) Binding parameters for BMP-2, BMP-4, and BMP-7 obtained from (a) Sebald et al. (2004), (b) Hatta et al. (2000), and (c) Rentzsch et al. (2006).

(E and F) Typical response curves show how the level of BR changes for increasing Cv-2 with different BMP concentrations for BMP-2 (E) and BMP-7 (F). See Table S1 for parameter values.

(G and H) The effect of cv-2 transfection or cv-2 RNAi on Dpp-mediated signaling (G) or Gbb-mediated signaling (H) in S2 cells. Signaling is measured by the relative levels of Flag-tagged Mad (green) and pMad (red), and is quantified in the histograms. Error bars are \pm the standard error of the mean.

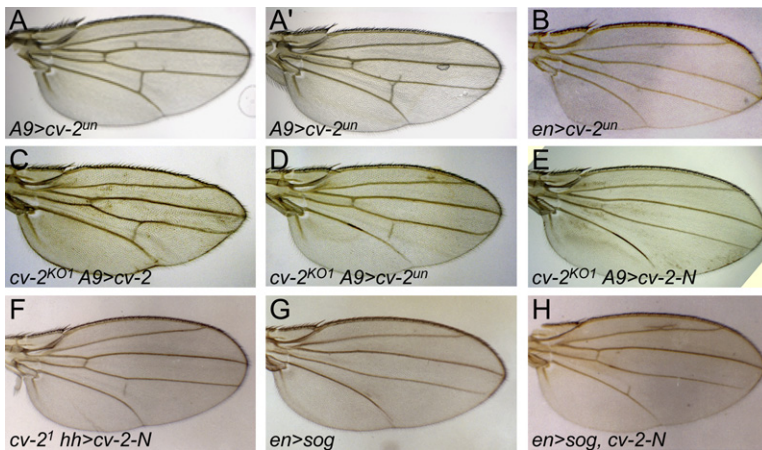


Figure 6. Comparison of the Effects of Cv-2 Variants on Adult Wings

(A and A') Mild overexpression of uncleavable Cv-2 with *A9-gal4*.

(B) Strong overexpression of uncleavable Cv-2 with *en-gal4*.

(C–E) Rescue of PCV loss in *cv-2^{KO1}* adults by *A9-gal4*-driven expression of wild-type *cv-2* (C) and uncleavable *cv-2* (D), but not by *cv-2-N* (E).

(F–H) Rescue of the PCV loss normally caused by either *cv-2¹* (F) or overexpression of Sog (G and H) by *en-gal4*-driven expression of Cv-2-N.

Because Cv-2 and type I receptors can co-IP independent of BMPs, we extended our model to include formation of a Cv-2/receptor complex and the binding of BMP to that complex (Figures S7 and S8). This addition did not significantly change the response to Cv-2, although it did in many cases lead to more pronounced biphasic responses. Moreover, it did not change the tendency to generate biphasic or antagonistic responses with BMP-7 or BMP-2, respectively. Our modeling suggests that Cv-2 might exhibit a more consistently biphasic activity with Gbb than with Dpp.

To test this we used an in vitro signaling assay. S2 cells respond to exogenous BMPs by phosphorylating transiently transfected Flag-tagged Mad. S2 cells also produce endogenous Cv-2, and the levels can thus be lowered by RNAi or raised by adding Cv-2 protein. We found that adding Cv-2 inhibited, but did not detectably promote, Dpp signaling over a wide range of Cv-2 and Dpp concentrations. Reducing *cv-2* by RNAi only increased Dpp signaling, indicating that endogenous Cv-2 antagonizes Dpp signaling in S2 cells (Figure 5G). Thus, in vitro the effects of Cv-2 on Dpp signaling are purely antagonistic. In contrast, the effects of Cv-2 on Gbb signaling in vitro were biphasic: reducing the levels of endogenous Cv-2 by RNAi treatment of S2 cells reduced Gbb signaling by 20%–30% for multiple Gbb concentrations tested, while adding Cv-2 also decreased signaling (Figure 5H). Thus, in otherwise identical in vitro settings, the effects of Cv-2 on BMP signaling depend on the type of the BMP ligand used.

Cleavage of Cv-2 Is Not Required to Promote BMP Signaling

It was recently proposed by Rentzsch et al. (2006) that the cleavage of Cv-2 into linked N-terminal and C-terminal fragments converts it from a form that inhibits BMP signaling into a form that promotes signaling. However, both cleaved and uncleaved forms of *Drosophila* Cv-2 interacted with the HSPG Dally (Figures 3C–3E) and with Tkv (Figure 3I and Figure S4A). While the cleavage of Cv-2 appears to lower its affinity for Dpp and Gbb (Figures 2J and 2K), our model predicts that cleaved Cv-2 is more likely to antagonize, rather than promote, signaling (66% biphasic solutions for HLL versus 28% for LLL in Figures 5A–5C).

We therefore compared the signaling abilities of full-length, cleavable Cv-2 and the uncleavable forms in vitro and in vivo.

As with the cleavable form, expressing moderate levels of the uncleavable form using the *A9-gal4* driver gave occasional ectopic venation consistent with a mild gain in BMP signaling (Figure 6A) and was able to rescue PCV formation in *cv-2^{KO1}* (Figure 6D) and *cv-2^{F1-42}* homozygotes (data not shown). Expressing even higher levels with *en-gal4*, however, inhibited PCV formation (Figure 6B). Thus, both cleavable and uncleavable Cv-2 have biphasic effects on BMP signaling.

The disulfide link between the two halves of Cv-2 forms before cleavage (Figure 2H), and there is no evidence from nonreducing western blots that fragments resembling Cv-2-N or Cv-2-C are released from that linkage (Figures 2E and 2F; Binnerts et al., 2004; Rentzsch et al., 2006). Since removing either the CR or vWFD domains severely reduces Cv-2's ability to bind BMPs (Figure 2L), these fragments would likely have reduced activity in vivo. Unlike wild-type and uncleavable Cv-2, Cv-2-N did not rescue the PCV loss observed in *cv-2^{KO1}* homozygotes when driven with *A9-gal4* (Figure 6E), despite being expressed at similar levels (data not shown). A GFP-tagged version of Cv-2-N can promote BMP signaling, but only weakly; it could not rescue *cv-2^{F1-42}*, but when driven at high levels with *hh-gal4* it partially rescued PCV formation in the *cv-2¹* hypomorph and partially rescued loss of PCV caused by overexpression of *UAS-sog* (Figures 6F and 6H). Neither form of Cv-2-N inhibited BMP signaling with any of a number of *gal4* drivers. We conclude that Cv-2-N is less effective at both promoting and inhibiting BMP signaling than the full-length cleavable or uncleavable forms.

cv-2 Expression Is Promoted by BMP Signaling

We previously showed that *cv-2* expression is heightened in late third instar discs near the anterior-posterior compartment boundary. In pupal stages, this emphasis is lost, but expression is heightened around the forming anterior and posterior crossveins (ACV and PCV) and along the distal tips of the longitudinal veins (Conley et al., 2000; Figures 7A–7C). These regions correspond with regions of heightened BMP signaling (Conley et al., 2000). Intriguingly, expression of *cv-2* is also heightened along the dorsal side of early *Drosophila* embryo, another region of enhanced BMP signaling (Figure 7D; Biemar et al., 2006).

We therefore tested whether *cv-2* expression is regulated by BMP signaling. Mutations in *cv* and *gbb* block BMP signaling in the developing PCV during pupal development but often leave

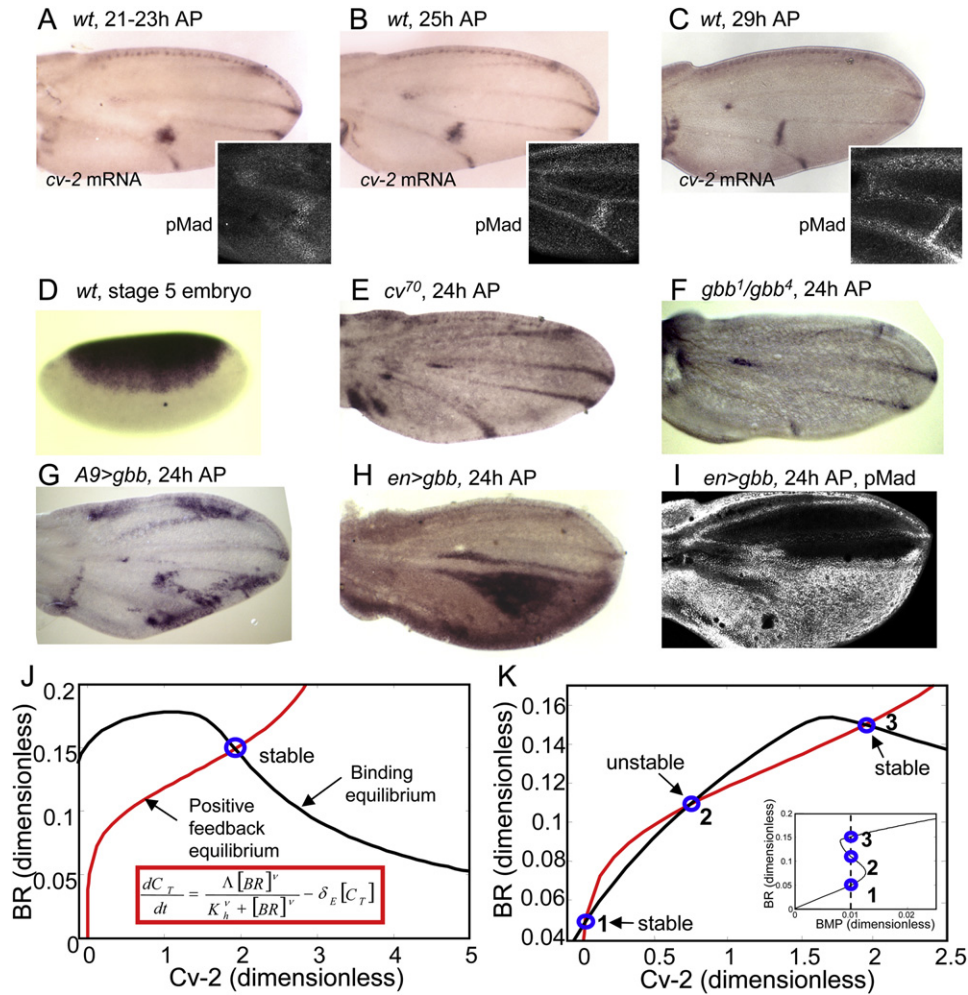


Figure 7. Positive Feedback of BMP Signaling on *cv-2* mRNA Expression

(A–C) Refinement of *cv-2* mRNA expression and anti-pMad staining in pupal wings. AP, after pupariation.

(D) Expression of *cv-2* in a stage 5 embryo.

(E and F) Loss of *cv-2* expression from regions of *cv⁷⁰* (E) and *gbb¹/gbb⁴* (F) pupal wings.

(G) *cv-2* expression after overexpression of moderate levels of Gbb with *A9-gal4*.

(H and I) *cv-2* expression (H) and anti-pMad staining (I) after overexpression of high levels of Gbb in the posterior of the wing with *en-gal4*.

(J) If Cv-2 acts as a strict antagonist, there is a single intersection between the binding and the positive feedback equilibria. See Table S1 for parameter values.

(K) If Cv-2 is biphasic, there are multiple intersections between the binding and positive feedback and equilibria, leading to bistability. The inset shows the bistable behavior as a function of the level of BMP. Points 1 and 3 are the stable steady states whereas point 2 is unstable. Additional analysis of the full 4D system shows the dynamic approach to the stable steady state (Umulis et al., 2006).

signaling in part of the ACV and the tips of the longitudinal veins intact (Shimmi et al., 2005a). Indeed, we found that *cv-2* expression was lost from the PCV in these mutants but remained in the distal tips and ACV (Figures 7E and 7F). Conversely, ectopic BMP signaling resulting from *A9-gal4*- or *en-gal4*-driven *UAS-gbb* induced high levels of pMad and *cv-2* expression throughout the posterior compartment, although *cv-2* exhibited a regional bias (Figures 7G and 7H) compared to pMad (Figure 7I). Thus, BMP signaling integrates with other patterning inputs to promote *cv-2* expression.

This positive feedback likely plays a role in refining the initially broad region of BMP signaling and *cv-2* expression observed at early stages of PCV development to the more tightly focused signaling observed at later stages (Figures 7A–7C; Conley

et al., 2000). In a previous model, it was shown that BMP-dependent induction of a cell surface BMP binding protein can lead to production of a bistable signaling state, i.e., a situation where there is an extremely sharp transition between cells that receive a very low and very high level of signal (Umulis et al., 2006). We explored this in more detail and found that the kinetics that lead to bistability depend on biphasic Cv-2 activity. If all cell surface complexes are internalized at the same rate, the balance between production and endocytosis (Figure 7J inset) determines the total amount of Cv-2 (C_T). We assume that *cv-2* expression shows a Hill-type saturation typical of many genes, with a maximum rate λ , a half maximal concentration K_h , and a cooperativity parameter v . The red lines in Figures 7J and 7K show the steady-state distribution of BMP-bound receptor (*BR*) for a given level of

Cv-2, and the intersections of the red lines with the black lines are the equilibrium solutions for Equations (1)–(3) when coupled with positive feedback. If Cv-2 can only antagonize signaling, there is one stable steady state (Figure 7J), but if the response to Cv-2 is biphasic, it can give rise to multiple steady states: two stable and one unstable state (Figure 7K). Since two stable states are separated by an unstable state, the system is considered bistable, and the specific state of the system depends on the current and previous states of the system. In the context of crossvein formation, bistability likely leads to sharp differences in pMad signaling between adjacent cells and a dynamic refinement of pMad accumulation as cells at the upper stable state out-compete adjacent cells for limited amounts of ligand, thus reinforcing the low signaling state of neighbors (Figure 7K and Umulis et al. 2006).

The binding of Cv-2 to cell surfaces, via the HSPGs and Tkv, also make it ideally suited to regulate and refine the region of BMP signaling. While a more diffusible molecule can increase signaling via positive feedback, our modeling shows that it would be much less effective at refining the boundaries of high signaling (Figure S9).

Lastly, incorporating positive feedback can explain a previous finding. Overexpression of Sog blocks signaling in the PCV, likely because excess Sog sequesters BMPs from receptors, while coexpression of low to moderate levels of Cv-2 rescues signaling in the PCV (Ralston and Blair, 2005). This result can be readily explained by an expanded version of our model that includes Sog and two new conservation conditions for the total level of BMP ligand and the total level of Sog in the system (Figure S10). In the expanded model, increasing the level of Sog shifts binding equilibrium curve maxima down and to the right. Signaling (BR) is dramatically reduced both by reduced levels of free BMP and the reduced positive feedback on *cv-2* expression (points 1 to 2 in Figure S10). Overexpression of Cv-2, however, shifts the positive-feedback curve to the right, and a new equilibrium is established with restored levels of BR (points 2 to 3 in Figure S10).

DISCUSSION

Here we showed that Cv-2 modulates BMP signaling in the *Drosophila* wing by a mechanism distinct from that of Sog. BMP signaling in the early stages of PCV development depends, in large part, on BMPs being produced in the adjacent longitudinal veins (Ray and Wharton, 2001; Ralston and Blair, 2005), and endogenous Sog acts over a long range to promote signaling in this context, likely by transporting BMPs from the longitudinal veins into the PCV region (Serpe et al., 2005; Shimmi et al., 2005a). Both Sog and Cv-2 are biphasic, as low levels promote and high levels inhibit BMP signaling. However, Cv-2 acts over a short range within the PCV, precluding a direct role in the long-range transport of ligands from the longitudinal veins. The short-range action of Cv-2 is likely to involve binding to cell surface proteins such as Dally, and strongly suggests that Cv-2 acts on cells receiving the BMP signal. Moreover, Cv-2 can stimulate signaling in vitro, where the transport or stability of BMPs in the medium is unlikely to be an issue (see also Kamimura et al., 2004; Ikeya et al., 2006).

Consistent with a role in reception, we found that Cv-2 binds not only BMPs, but also the type I BMP receptor Tkv and verte-

brate BMPR-IA and -IB. We therefore propose that the binding between Cv-2 and receptor facilitates transfer and signaling of BMPs via formation of a transient, nonsignaling complex containing Cv-2, type I receptor, and BMPs. We propose that at moderate levels, Cv-2 moves ligand from the extracellular space onto receptors via this complex, while at higher levels Cv-2 antagonizes signaling by sequestering ligand in the complex. The inability of this complex to signal is consistent with studies suggesting that Cv-2 binds to the BMP “knuckle” epitope used to bind type II BMP receptors (Zhang et al., 2007).

Our computational analyses also predict that the relative affinities of different BMPs for Cv-2 or receptors will influence the effect of Cv-2 upon signaling. Although the vertebrate counterparts of BMP ligands appear to have similar affinities for Cv-2, they have different affinities for their receptors, and our model predicts that this alone can alter the activity of Cv-2. Indeed, we find that in cell culture assays Cv-2 only antagonizes Dpp signaling, but has biphasic effects on Gbb signaling. This could explain why a vertebrate member of the Cv-2/Kielin-like family, mouse KCP, stimulates BMP-2 signaling but inhibits TGF- β and Activin signaling in vitro (Lin et al., 2005, 2006). Likewise, in the early *Drosophila* embryo, where a different set of BMP ligands act, we have found that loss of endogenous *cv-2* actually expands BMP signaling, opposite to the effects of Cv-2 loss in the PCV (Y.-C. Wang, M.S., C. Brakken-Thal, M.B.O., and E. Ferguson, unpublished data). Thus, Cv-2 activity is highly context dependent.

Fundamental to our model is the formation of a transient complex containing Cv-2, BMP, and the receptor. Tripartite complexes have been demonstrated to form between follistatin, type I receptor, and BMP ligands (Iemura et al., 1998), and we have found that Cv-2 and the extracellular portion of BMPR-IB simultaneously coimmunoprecipitate with Dpp. Similarly, the vertebrate type I receptor can coprecipitate both BMP and mouse KCP (Lin et al., 2005). Although we have not been able to directly demonstrate the tripartite intermediate, this might reflect the transient nature of this complex due to very rapid on-off kinetics. In fact, our modeling predicts the intermediate is a low-affinity, transient complex.

It is important to recognize that Cv-2 does not act as an obligate coreceptor in our model. Rather, Cv-2 is modulatory, consistent with the fact that Cv-2 does not participate in BMP signaling in many contexts. In fact, our model requires that the tripartite complex does not signal, and it is only after Cv-2 is displaced that the type I receptor is free to signal. This is in contrast to the activity of coreceptors like Cripto, which is required for binding of the TGF- β family member Nodal to type I receptors and formation of signaling complexes with type II receptors (Yeo and Whitman, 2001). While Cripto can antagonize signaling, this involves non-Nodal ligands (Gray et al., 2006). In contrast, Cv-2 can promote or antagonize the signaling mediated by a single type of ligand such as Gbb.

Comparison to Vertebrate Cv-2

The functional, structural, and regulatory aspects of *Drosophila* Cv-2 show remarkable conservation with its vertebrate homologs in terms of HSPG binding, cleavage, and feedback by BMP signaling (Binnerts et al., 2004; Coffinier et al., 2002; Coles et al., 2004; Ikeya et al., 2006; Kamimura et al., 2004; Moser

et al., 2003, 2007; Rentzsch et al., 2006). Despite these similarities, a different mechanism was recently proposed to explain the ability of zebrafish Cv-2 to either promote or inhibit signaling; the cleavage of Cv-2 was proposed to convert Cv-2 from an antagonist to an agonist (Rentzsch et al., 2006). In support of this model was the observation that an uncleavable form of Cv-2 was more potent at dorsalizing zebrafish embryos (indicating a loss of BMP signaling) than was the full-length cleavable form, and that an N-terminal fragment lacking the vWFD domain ventralized embryos (indicating a gain in BMP signaling). Processing did not dramatically alter the K_D of zebrafish Cv-2 for BMP binding, but apparently blocked its ability to bind HSPGs. Thus, the authors proposed that uncleaved Cv-2 binds HSPGs to sequester BMPs, while cleaved Cv-2 promoted signaling in a tissue-specific manner by an unknown mechanism.

We found little support for this model in *Drosophila*. Blocking cleavage did not create a strictly inhibitory molecule, since both wild-type and uncleavable *Drosophila* Cv-2 acted in a biphasic fashion. Moreover, both cleaved and uncleaved forms of *Drosophila* Cv-2 bound Dally and cell surfaces (Figures 3C–3E). We also did not find evidence of differential cleavage among cell types or developmental stages. Evidence from other secreted proteins suggests that GD-PH cleavages like that in Cv-2 occur via an autocatalytic process triggered by the low pH found within the late secretory compartments (Thuveson and Fries, 2000). Indeed, we found evidence of constitutive, pH-dependent Cv-2 cleavage in vitro (M.S. and M.B.O., unpublished data), suggestive of an unpatterned, autocatalytic process in vivo.

Nonetheless, conservation of the cleavage site among species suggests that cleavage plays an important role, and we found that cleavage of *Drosophila* Cv-2 lowers its affinity for BMPs in vitro. However, similar manipulations of zebrafish Cv-2 did not greatly affect its K_D for BMP (Rentzsch et al., 2006; Zhang et al., 2007). These may represent true species-specific differences, or they may result from differences in the binding assays used: the immobilization of proteins in the Biacore analyses of zebrafish Cv-2, or the presence of additional factors in the conditioned S2 cell medium present in coimmunoprecipitation assays. Since *Drosophila* Cv-2 can rescue the knockdown of zebrafish Cv-2 (Rentzsch et al., 2006), any species-specific differences are likely quantitative, rather than qualitative.

A Role for Sog/Chordin?

In zebrafish, Chordin largely antagonizes BMP signaling, and thus Cv-2 and Chordin have essentially opposite effects on BMP signaling. However, loss of Cv-2 ameliorates only a subset of the gain-of-signaling phenotypes caused by loss of Chordin (Rentzsch et al., 2006). Thus, Cv-2 has been proposed to promote signaling by two distinct mechanisms, one that depends on Chordin and one that is independent of Chordin. Our model can explain the Chordin-independent effect of Cv-2 and suggests that the Chordin-dependent effect may result from competition between Chordin and Cv-2 for BMPs. Since Cv-2 can block binding between BMPs and Chordin (Rentzsch et al., 2006), the presence of Cv-2 will impact the amount of Chordin-bound BMP. In the absence of Chordin, the amount of free BMPs is likely to be higher, and the effect of Cv-2 in promoting signaling would not be as prominent.

The situation is different in the *Drosophila* wing, where both Sog and Cv-2 promote signaling in the developing PCV. A model has emerged, from our studies and others', in which Sog and Cv (Tsg2) facilitate transport of BMPs into the PCV competent zone, where processing by Tlr leads to release of BMPs, and capture by Cv-2 for presentation to receptors. Thus, Sog and Cv-2 act coordinately, through independent mechanisms, to promote BMP signaling during PCV specification. Intriguingly, we have also observed binding between Cv-2 and Sog in vitro (D.J.O., S.M. Honeyager, and S.S.B., unpublished data), and this may provide a direct connection between the two systems by facilitating the exchange of BMPs from Sog to Cv-2 and thus onto the receptor.

Conclusions

The data we present here indicate that Cv-2 can have remarkably versatile effects on signaling depending on the particular context in which it acts, providing an explanation for the contradictory effects observed for members of Cv-2/Kielin family in different developmental contexts. In addition, we demonstrate that coupling the extracellular effects with positive feedback on the production of Cv-2 itself can lead to bistable signaling wherein a very sharp transition can be generated between cells that receive high versus low levels of signal. This positive feedback thus provides a mechanism for positionally refining signaling. However, the ability of Cv-2 to promote signaling apparently does not rely solely on spatial patterns of Cv-2, Sog, and Cv expression: Cv-2 promotes signaling in cell culture (Figure 4H; Kamimura et al., 2004; Ikeya et al., 2006), and the PCV is formed in wings in which Cv-2, Sog, and Cv are overexpressed throughout the posterior compartment (Ralston, 2004; Ralston and Blair, 2005; O'Connor et al., 2006). Our model of Cv-2 function shows how a cell surface ligand-binding molecule can act locally to either promote or inhibit signaling. We note that this model may be applicable to other molecules such as the HSPGs that have been proposed to both activate and inhibit signaling (Fujise et al., 2001).

EXPERIMENTAL PROCEDURES

Molecular Constructs, Fly Stocks, and Clonal Analyses

See the Supplemental Data.

Immunohistochemistry and RNA Localization

In situ hybridization and immunohistochemistry of wing discs or pupal wings was performed as previously described (Ralston and Blair, 2005), except in some cases we used a rabbit anti-pSmad (1/2500) kindly provided by Dan Vasiliaskas, Susan Morton, Tom Jessell, and Ed Laufer.

For extracellular staining unfixed late third instar wing discs were incubated for 1 hr on ice in PBS containing 1:300 mouse anti-Myc (Santa Cruz), washed for 1–5 min in PBS, and then fixed in 4% formaldehyde in PBS, washed, and stained with secondary antibodies. Some discs were counterstained after fixation with 1:20 rat anti-Ci or 1/200 rat anti-HA 3F10 (Roche).

S2 cells were transiently transfected with Dally-Myc, grown for 4 days in serum-free M3, then attached to concanavalinA-coated slides for 1 hr at 25°C and washed for 15 min in ice-cold M3. The attached cells were incubated with conditioned media (see below) containing V5-tagged Cv-2 variants for 1 hr at 4°C, washed for 15 min in ice-cold M3, and fixed in 4% formaldehyde in PBS. Cells were stained with rabbit anti-Myc antibody (Santa Cruz) 1:1000 and mouse anti-V5 (Invitrogen) 1:200, followed by secondary antibodies (Molecular Probes), and then mounted in Vectashield containing DAPI (Vector Laboratories).

Protein Production and Detection

Drosophila S2 and S2* cells were used for producing recombinant proteins in vitro as described previously (Shimmi and O'Connor, 2003; Serpe et al., 2005). In vivo Cv-2 was isolated from embryos sheared in lysis buffer (PBS with 0.9 M glycerol, 1% Triton X-100, 0.5 mM DTT, and protease inhibitor cocktail [Roche]), incubated on ice for 30 min, and centrifuged at 14,000 rpm for 15 min at 4°C, and the soluble phase was analyzed by western.

For sequencing, the C-terminal half of Cv-2 was purified by first fractionating the conditioned medium on an S-Sepharose column by HPLC and dialyzing the desired fractions in the presence of Ni-NTA-Agarose (QIAGEN). The Cv-2-bound beads were washed and resuspended in SDS-loading buffer, and the material was resolved on a preparative gel. A major 55 kDa band was isolated and analyzed at Harvard Microchemical Facilities.

For western blotting, primary antibodies were used at the following dilutions: rabbit anti-Myc A14 (Santa Cruz) 1:1000, anti-V5 (Invitrogen) 1:5000, anti-HA 12CA5 (Roche) 1:2000, anti-Flag M2 (Sigma) 1:2000, anti-penta His (QIAGEN) 1:2000, and anti-Dpp (R&D Systems) 1:2000. Immune complexes were visualized with secondary antibodies IRDye 700 and 800 at 1:5000 followed by scanning with Odyssey Infrared Imaging System (Li-Cor Biosciences), or by using HRP secondary antibodies (Jackson) visualized with Pierce SuperSignal West. Recombinant chimeric receptors (BMPr-IB/, BMPr-II/, and ErbB2/Fc) and recombinant Dpp were from R&D Systems.

Cell-Based Assays

The signaling assay for BMP signaling was described previously (Shimmi and O'Connor, 2003; Zheng et al., 2003). For cell binding assays, naive or transiently transfected S2 cells were attached to concanavalin A-coated slides or collected in test tubes and presented with Cv-2 protein variants. After incubation, cells were washed and then lysed by boiling in SDS-loading buffer, and the lysates were analyzed by western. Alternatively, cells were lysed for 15 min on ice in lysis buffer (50 mM Tris [pH 7.5], 150 mM NaCl, 0.5% Tween-20, and protease inhibitor cocktail), and the lysates were cleared by centrifugation (10 min at 4°C) and then subjected to IP followed by western analysis.

Computational Analysis

Randomly chosen parameter values were varied over 4 orders of magnitude from 10^{-3} to 10^1 $\text{nM}^{-1}\text{min}^{-1}$ and from 10^{-2} to 10^2 min^{-1} for the forward and reverse reactions, respectively. BMP and receptor levels were varied from 10^{-2} nM to 10^2 nM for BMP and 10^1 to 10^4 nM for receptors, which covers the biologically relevant range for receptor and BMP levels (Shimmi et al., 2005b; Urmulis et al., 2006).

Steady-state solutions for Equations (1)–(4) were computed using a custom Newton-Raphson solver and the built-in nonlinear equation solver in Matlab. An initial guess for the nonlinear solver was obtained by solving the differential Equations (1)–(3) for long times using the built-in Matlab ODE solvers. Zeroth-order continuation was used to find the dependence of *BR* on Cv-2 for increasing levels of Cv-2. Solutions were sorted into three categories (biphasic, antagonistic, and nonphysical solutions) depending on the qualitative behavior of Cv-2 and the convergence properties. During the large-scale parameter variation, 3% of the solutions did not converge properly, or converged to a non-physical solution (such as a negative concentration). When plotted alongside the biphasic and antagonistic solutions, the nonconverged and nonphysical solutions did not show a bias toward a particular quadrant, but were biased (slightly) toward the region of parameter space corresponding to low values for K_{BCR} . Since the subset of solutions that did not converge represents a small fraction of the total solutions in each region of parameter space, they do not affect our conclusions.

SUPPLEMENTAL DATA

Supplemental Data include ten figures, one table, Supplemental Experimental Procedures, and Supplemental References and are available with this article online at <http://www.developmentalcell.com/cgi/content/full/14/6/940/DC1/>.

ACKNOWLEDGMENTS

This work was supported by grants from NSF (IBN0077912 and IBN0416586) and NIH (NS028202) to S.S.B. and from NIH (GM29123) to H.O. D.U. is sup-

ported by the NIH Biotechnology Training Grant. M.B.O. is an Investigator with the Howard Hughes Medical Institute. S.S.B. thanks S.M. Honeyager for technical assistance.

Received: June 6, 2007

Revised: December 4, 2007

Accepted: March 31, 2008

Published: June 9, 2008

REFERENCES

- Belenkaya, T.Y., Han, C., Yan, D., Opoka, R.J., Khodoun, M., Liu, H., and Lin, X. (2004). *Drosophila* Dpp morphogen movement is independent of dynamin-mediated endocytosis but regulated by the glypican members of heparan sulfate proteoglycans. *Cell* 119, 231–244.
- Biemar, F., Nix, D.A., Piel, J., Peterson, B., Ronshaugen, M., Sementchenko, V., Bell, I., Manak, J.R., and Levine, M.S. (2006). Comprehensive identification of *Drosophila* dorsal-ventral patterning genes using a whole-genome tiling array. *Proc. Natl. Acad. Sci. USA* 103, 12763–12768.
- Binnerts, M.E., Wen, X., Cante-Barrett, K., Bright, J., Chen, H.T., Asundi, V., Sattari, P., Tang, T., Boyle, B., Funk, W., et al. (2004). Human Crossveinless-2 is a novel inhibitor of bone morphogenetic proteins. *Biochem. Biophys. Res. Commun.* 315, 272–280.
- Coffinier, C., Ketpura, N., Tran, U., Geissert, D., and De Robertis, E.M. (2002). Mouse Crossveinless-2 is the vertebrate homolog of a *Drosophila* extracellular regulator of BMP signaling. *Mech. Dev.* 119 (Suppl 1), S179–S184.
- Coles, E., Christiansen, J., Economou, A., Bronner-Fraser, M., and Wilkinson, D.G. (2004). A vertebrate crossveinless 2 homologue modulates BMP activity and neural crest cell migration. *Development* 131, 5309–5317.
- Conley, C.A., Silburn, R., Singer, M.A., Ralston, A., Rohwer-Nutter, D., Olson, D.J., Gelbart, W., and Blair, S.S. (2000). Crossveinless 2 contains cysteine-rich domains and is required for high levels of BMP-like activity during the formation of the cross veins in *Drosophila*. *Development* 127, 3947–3959.
- Fujise, M., Izumi, S., Selleck, S.B., and Nakato, H. (2001). Regulation of dally, an integral membrane proteoglycan, and its function during adult sensory organ formation of *Drosophila*. *Dev. Biol.* 235, 433–448.
- Gray, P.C., Shani, G., Aung, K., Kelber, J., and Vale, W. (2006). Cripto binds transforming growth factor β (TGF- β) and inhibits TGF- β signaling. *Mol. Cell. Biol.* 26, 9268–9278.
- Han, C., Belenkaya, T.Y., Khodoun, M., Tauchi, M., Lin, X., and Lin, X. (2004). Distinct and collaborative roles of *Drosophila* EXT family proteins in morphogen signalling and gradient formation. *Development* 131, 1563–1575.
- Hatta, T., Konishi, H., Katoh, E., Natsume, T., Ueno, N., Kobayashi, Y., and Yamazaki, T. (2000). Identification of the ligand-binding site of the BMP type IA receptor for BMP-4. *Biopolymers* 55, 399–406.
- Iemura, S., Yamamoto, T.S., Takagi, C., Uchiyama, H., Natsume, T., Shimazaki, S., Sugino, H., and Ueno, N. (1998). Direct binding of follistatin to a complex of bone-morphogenetic protein and its receptor inhibits ventral and epidermal cell fates in early *Xenopus* embryo. *Proc. Natl. Acad. Sci. USA* 95, 9337–9342.
- Ikeya, M., Kawada, M., Kiyonari, H., Sasai, N., Nakao, K., Furuta, Y., and Sasai, Y. (2006). Essential pro-Bmp roles of crossveinless 2 in mouse organogenesis. *Development* 133, 4463–4473.
- Kamimura, M., Matsumoto, K., Koshiba-Takeuchi, K., and Ogura, T. (2004). Vertebrate crossveinless 2 is secreted and acts as an extracellular modulator of the BMP signaling cascade. *Dev. Dyn.* 230, 434–445.
- Lander, A.D. (2007). Morpheus unbound: reimagining the morphogen gradient. *Cell* 128, 245–256.
- Lin, X. (2004). Functions of heparan sulfate proteoglycans in cell signaling during development. *Development* 131, 6009–6021.
- Lin, J., Patel, S.R., Cheng, X., Cho, E.A., Levitan, I., Ullenbruch, M., Phan, S.H., Park, J.M., and Dressler, G.R. (2005). Kielin/chordin-like protein, a novel enhancer of BMP signaling, attenuates renal fibrotic disease. *Nat. Med.* 11, 387–393.

- Lin, J., Patel, S.R., Wang, M., and Dressler, G.R. (2006). The cysteine-rich domain protein KCP is a suppressor of transforming growth factor β /activin signaling in renal epithelia. *Mol. Cell. Biol.* **26**, 4577–4585.
- Marti, T., Rosselet, S.J., Titani, K., and Walsh, K.A. (1987). Identification of disulfide-bridged substructures within human von Willebrand factor. *Biochemistry* **26**, 8099–8109.
- Matsui, M., Mizuseki, K., Nakatani, J., Nakanishi, S., and Sasai, Y. (2000). *Xenopus* kielin: a dorsaling factor containing multiple chordin-type repeats secreted from the embryonic midline. *Proc. Natl. Acad. Sci. USA* **97**, 5291–5296.
- Moser, M., Binder, O., Wu, Y., Aitsebaomo, J., Ren, R., Bode, C., Bautch, V.L., Conlon, F.L., and Patterson, C. (2003). BMPER, a novel endothelial cell precursor-derived protein, antagonizes bone morphogenetic protein signaling and endothelial cell differentiation. *Mol. Cell. Biol.* **23**, 5664–5679.
- Moser, M., Yu, Q., Bode, C., Xiong, J.W., and Patterson, C. (2007). BMPER is a conserved regulator of hematopoietic and vascular development in zebrafish. *J. Mol. Cell. Cardiol.* **43**, 243–253.
- O'Connor, M.B., Umulis, D., Othmer, H.G., and Blair, S.S. (2006). Shaping BMP morphogen gradients in the *Drosophila* embryo and pupal wing. *Development* **133**, 183–193.
- Ralston, A. (2004). The roles of the cysteine-rich domain proteins Crossveinless 2, Short gastrulation, and Twisted gastrulation 2 during crossvein patterning in the wing of *Drosophila melanogaster*. PhD thesis, University of Wisconsin, Madison.
- Ralston, A., and Blair, S.S. (2005). Long-range Dpp signaling is regulated to restrict BMP signaling to a crossvein competent zone. *Dev. Biol.* **280**, 187–200.
- Ray, R.P., and Wharton, K.A. (2001). Context-dependent relationships between the BMPs *gbb* and *dpp* during development of the *Drosophila* wing imaginal disk. *Development* **128**, 3913–3925.
- Rentsch, F., Zhang, J., Kramer, C., Sebald, W., and Hammerschmidt, M. (2006). Crossveinless 2 is an essential positive feedback regulator of Bmp signaling during zebrafish gastrulation. *Development* **133**, 801–811.
- Sebald, W., Nickel, J., Zhang, J.L., and Mueller, T.D. (2004). Molecular recognition in bone morphogenetic protein (BMP)/receptor interaction. *Biol. Chem.* **385**, 697–710.
- Serpe, M., Ralston, A., Blair, S.S., and O'Connor, M.B. (2005). Matching catalytic activity to developmental function: Tollid-related processes Sog in order to help specify the posterior crossvein in the *Drosophila* wing. *Development* **132**, 2645–2656.
- Shimmi, O., and O'Connor, M.B. (2003). Physical properties of Tld, Sog, Tsg and Dpp protein interactions are predicted to help create a sharp boundary in Bmp signals during dorsoventral patterning of the *Drosophila* embryo. *Development* **130**, 4673–4682.
- Shimmi, O., Ralston, A., Blair, S.S., and O'Connor, M.B. (2005a). The crossveinless gene encodes a new member of the Twisted gastrulation family of BMP-binding proteins which, with Short gastrulation, promotes BMP signaling in the crossveins of the *Drosophila* wing. *Dev. Biol.* **282**, 70–83.
- Shimmi, O., Umulis, D., Othmer, H., and O'Connor, M.B. (2005b). Facilitated transport of a Dpp/Scw heterodimer by Sog/Tsg leads to robust patterning of the *Drosophila* blastoderm embryo. *Cell* **120**, 873–886.
- Strigini, M., and Cohen, S.M. (2000). Wingless gradient formation in the *Drosophila* wing. *Curr. Biol.* **10**, 293–300.
- Takei, Y., Ozawa, Y., Sato, M., Watanabe, A., and Tabata, T. (2004). Three *Drosophila* EXT genes shape morphogen gradients through synthesis of heparan sulfate proteoglycans. *Development* **131**, 73–82.
- Thuveson, M., and Fries, E. (2000). The low pH in trans-Golgi triggers autocatalytic cleavage of pre- α -inhibitor heavy chain precursor. *J. Biol. Chem.* **275**, 30996–31000.
- Umulis, D.M., Serpe, M., O'Connor, M.B., and Othmer, H.G. (2006). Robust, bistable patterning of the dorsal surface of the *Drosophila* embryo. *Proc. Natl. Acad. Sci. USA* **103**, 11613–11618.
- Vilmos, P., Sousa-Neves, R., Lukacsovich, T., and Marsh, J.L. (2005). crossveinless defines a new family of Twisted-gastrulation-like modulators of bone morphogenetic protein signalling. *EMBO Rep.* **6**, 262–267.
- Wang, Y.C., and Ferguson, E.L. (2005). Spatial bistability of Dpp-receptor interactions during *Drosophila* dorsal-ventral patterning. *Nature* **434**, 229–234.
- Yeo, C., and Whitman, M. (2001). Nodal signals to Smads through Cripto-dependent and Cripto-independent mechanisms. *Mol. Cell* **7**, 949–957.
- Zhang, J.L., Huang, Y., Qiu, L.Y., Nickel, J., and Sebald, W. (2007). von Willebrand factor type C domain-containing proteins regulate bone morphogenetic protein signaling through different recognition mechanisms. *J. Biol. Chem.* **282**, 20002–20014.
- Zheng, X., Wang, J., Haerry, T.E., Wu, A.Y., Martin, J., O'Connor, M.B., Lee, C.H., and Lee, T. (2003). TGF-beta signaling activates steroid hormone receptor expression during neuronal remodeling in the *Drosophila* brain. *Cell* **112**, 303–315.